Continuum-Based Voronoi Tessellated Models for Capturing Unloading-Induced Brittle Damage in Hard Rocks

Fatemeh Amiri(✉) and Navid Bahrani

Dalhousie University, Halifax, NS, Canada
fatima.amiri@dal.ca

Abstract. The continuum numerical program RS2 was used to generate a Voronoi Tessellated Model (VTM), consisting of blocks meshed into several triangular elements and block boundaries simulated using joint elements. The RS2-VTM was calibrated to the compressive and tensile strengths of undamaged Lac du Bonnet (LdB) granite. The simulation results indicated a reasonable agreement between the peak strength and post-peak response of the RS2-VTM and those of LdB granite. Next, simplified 3D coring stress paths for horizontal and vertical boreholes at the 420 level of Canada's Underground Research Laboratory (URL) were applied to the calibrated RS2-VTM. The simulated core damage (i.e., yielded joint elements in RS2) was found to be comparable to that of discontinuum models. Finally, 2D and 3D stress paths experienced by the rock mass in the roof of the Mine-by Experiment (MBE) tunnel at the URL were applied to the calibrated RS2-VTM. It was found that the 3D stress path causes more damage compared to the 2D stress path due to the tensile stress generated ahead of the MBE tunnel face, which is not captured in 2D models.

Keywords: Core damage · Unloading-induced stress path · Hard brittle rock · Voronoi Tessellated Model (VTM)

1 Introduction

At different design stages of underground excavations, core samples obtained by drilling are used to determine geotechnical design parameters, such as the Unconfined Compressive Strength (UCS) and Young's modulus (E) of intact rock. Previous research has shown that when core samples are retrieved from high-stress environments, damage to the core in the form of micro-cracks may result in incorrect estimation of these parameters. Martin and Stimpson [1] reported that core damage affected the laboratory properties of Lac du Bonnet (LdB) granite cores retrieved from the 420 level of the Underground Research Laboratory (URL) in Manitoba, Canada. The observed damage is believed to be due to the complex stress paths experienced by the core during drilling [2]. The v-shaped notch failure around the Mine-by Experiment (MBE) tunnel at the 420 level of the URL was also attributed to the complex stress path experienced by the rock near the excavation boundary during the tunnel advance [3].

R. E. Hammah et al. (Eds.): RIC 2023, AHE 19, pp. 137–145, 2023.
https://doi.org/10.2991/978-94-6463-258-3_14

Previous studies have emphasized the need to incorporate grain-scale heterogeneities into numerical models to capture the failure process of brittle rocks [e.g., 4]. This is achieved by generating a grain-like structure of brittle rocks using a Discrete Fracture Network (DFN). The built-in Voronoi joint network in RS2 (by Rocscience), which is a commercial numerical program based on the implicit Finite Element Method (FEM), can be used to generate polygonal grain-like structures. This model, called a Voronoi Tessellated Model (VTM), comprises blocks and block boundaries. Properties of the blocks and block boundaries (called micro-properties) are adjusted through an iterative process known as the 'calibration' until the macro-properties and macro-behavior of the VTM match those of rock specimens obtained from laboratory tests.

The central objective of this research is to investigate the effect of core drilling and tunnel excavation stress paths on brittle damage in hard rocks using a continuum-based VTM. For this purpose, an RS2-VTM is first calibrated to the laboratory properties of undamaged LdB granite. Simplified 3D coring and tunnel excavation stress paths are then applied to the calibrated model to simulate unloading-induced brittle damage.

2 Continuum-Based VTM of Lac Du Bonnet Granite

In an RS2-VTM, the Voronoi blocks consist of several triangular mesh elements, and the block boundaries are simulated using joint elements [4]. In this research, the built-in joint network option in RS2 was used to generate Voronoi blocks within the model domain using open-ended joint elements with an average length of 2.5 mm. Figure 1 shows the boundary conditions of RS2-VTMs used to simulate unconfined compression (Fig. 1a), confined compression (Fig. 1b), direct tensile (Fig. 1c) and Brazilian tensile (Fig. 1d) tests. Table 1 summarizes the macro-properties of undamaged LdB granite, which were the targets for the RS2-VTM calibration.

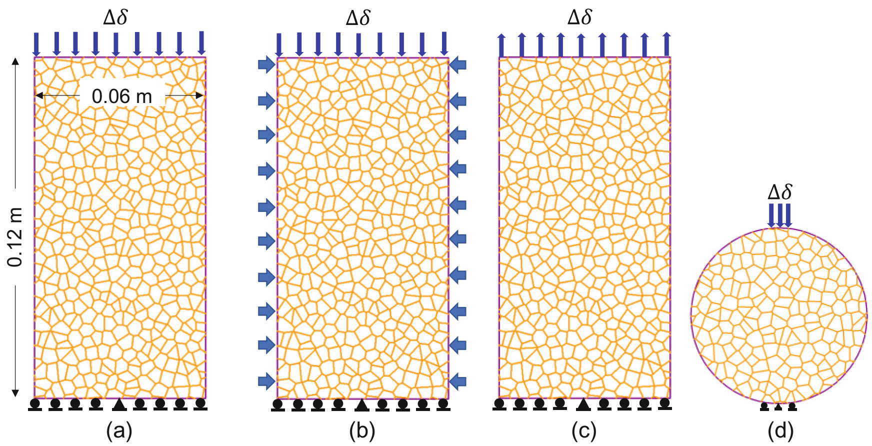

Fig. 1. Boundary conditions in RS2-VTM used to simulate laboratory tests: a) unconfined compression; b) confined compression; c) direct tensile; and d) Brazilian tensile tests.

Table 1. Summary of laboratory properties of LdB granite [5]

Young's modulus (GPa)	Poisson's ratio	Friction angle (°)	Cohesion (MPa)	Brazilian Tensile strength (MPa)	Direct Tensile strength (MPa)
69 ± 5.8	0.26 ± 0.04	59	30	9.3 ± 1.3	6.9

There are 16 unknown input parameters (micro-properties) in an RS2-VTM: peak and residual cohesion, friction angle, and tensile strength, and Young's modulus and Poisson's ratio for blocks (i.e., mesh elements); peak and residual cohesion, friction angle, and tensile strength, and normal and shear stiffness for block boundaries (i.e., joint elements). To simplify the calibration process, some assumptions were made to reduce the number of unknown micro-properties, as described below:

- RS2-VTM consists of only one mineral type.
- The elastic properties of the blocks in the RS2-VTM are equal to the weighted average of those for four main mineral types in LdB granite (i.e., E = 78 GPa and $\upsilon = 0.22$).
- The block boundary (joint) stiffness ratio (k_n/k_s) is 2.5.
- The residual tensile strength of the blocks and block boundaries is 0.1 MPa.
- The residual cohesion of the blocks and block boundaries is 0.1 MPa.
- The peak and residual friction angles of the blocks and block boundaries are equal to that of LdB granite obtained from laboratory triaxial tests (i.e., 59°).

Based on the above assumptions, the number of unknown micro-properties was reduced from 16 to 7. Table 2 shows the micro-properties of the calibrated RS2-VTM. Note that Sanipour et al. [6] also calibrated an RS2-VTM to the laboratory properties of undamaged LdB granite. They used the calibrated model to simulate the v-shaped notch failure around the Mine-by Experiment (MBE) tunnel at the URL. The calibration presented in this study differs from that of Sanipour et al. [6] in the following:

- The specimen size for the test simulations matches the dimensions of standard laboratory specimens.
- The RS2-VTM was calibrated to the peak strength of LdB granite for the full range of confinement (0–60 MPa).
- The post-peak behavior and residual strength of LdB granite in the confined compression tests were considered in the calibration.
- The direct to Brazilian tensile strength ratio of LdB granite (i.e., 0.75) was considered in the calibration.

Figure 2 demonstrates the results of unconfined and confined compressive test simulations including the stress-strain curves and failure modes. As can be seen in Fig. 2b, LdB granite exhibits a brittle post-peak behavior even at high confining pressures (e.g., $\sigma_3 = 60$ MPa). The assumed 0.1 MPa for the block residual cohesion in the RS2-VTM allowed for capturing the observed post-peak response in the confined compression tests.

Figure 3a depicts the peak strengths of the calibrated RS2-VTM at different confining pressures, demonstrating a reasonable agreement with the Hoek-Brown strength

Table 2. Micro-properties of the calibrated RS2-VTM.

Micro-properties		Block	Block boundary
Peak strength	Cohesion (MPa)	82	45
	Friction angle (°)	59	59
	Tensile strength (MPa)	22	9.8
Residual strength	Cohesion (MPa)	0.1	0.1
	Friction angle (°)	59	59
	Tensile strength (MPa)	0.1	0.1
Deformation properties	Young's modulus (GPa)	78	-
	Poisson's ratio	0.22	-
	Normal stiffness (GPa/m)	-	145,000
	Shear stiffness (GPa/m)	-	58,000

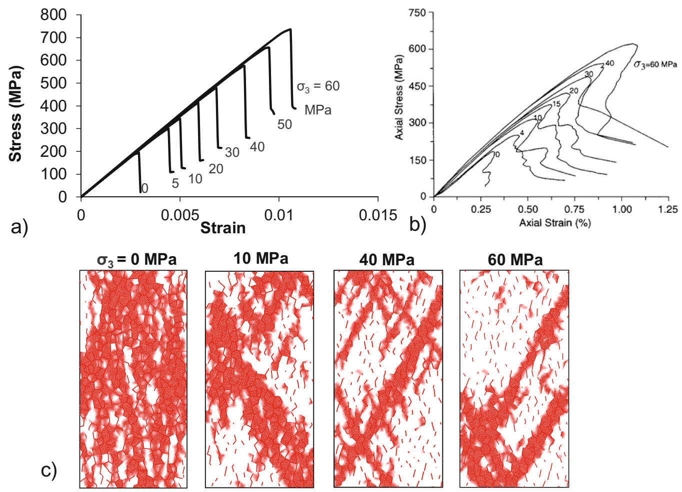

Fig. 2. Stress-strain curves of: a) RS2-VTM; and b) LdB granite [3]. c) Simulated failure modes in unconfined and confined compression tests

envelope fitted to the laboratory triaxial test data for undamaged LdB granite. The peak and residual strengths from the stress-strain curves in Fig. 2a–b were digitized and plotted in Fig. 3b. As can be seen in this figure, the residual strengths of LdB granite are well captured by the RS2-VTM, using an assumed block residual cohesion of 0.1 MPa.

Figure 4a shows the stress-strain curves and failure modes obtained from the Brazilian and direct tensile test simulations. The simulation results (i.e., post-peak response and failure modes) are consistent with those of laboratory tests on granite [7]. The direct and Brazilian tensile test simulations resulted in tensile strengths of 6.9 MPa and

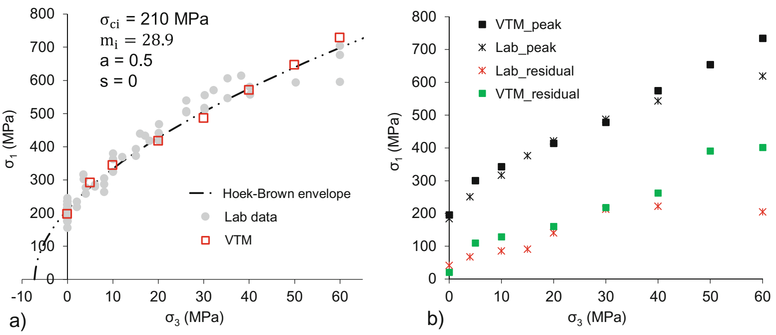

Fig. 3. Comparison between: a) RS2-VTM peak strengths and Hoek-Brown failure envelope fitted to the LdB granite triaxial test data [3]; and b) RS2-VTM and LdB granite peak and post-peak strengths

9.2 MPa, respectively, which are comparable to the laboratory-measured tensile strengths for undamaged LdB granite [5].

It should be noted that the average of node stresses within the RS2-VTM was used to determine the tensile stress in the direct tensile test simulation. However, in the Brazilian test simulation, the sum of reaction forces at the upper specimen boundary was used in the following equation to calculate the tensile stresses [8].

$$\sigma_t = \frac{2F}{\pi Dt} \tag{1}$$

In the equation, D is the specimen diameter, t is the thickness, and F is the sum of reaction forces in N. In the simulated Brazilian test, D was 0.06 m, and t was assumed to be 1 m.

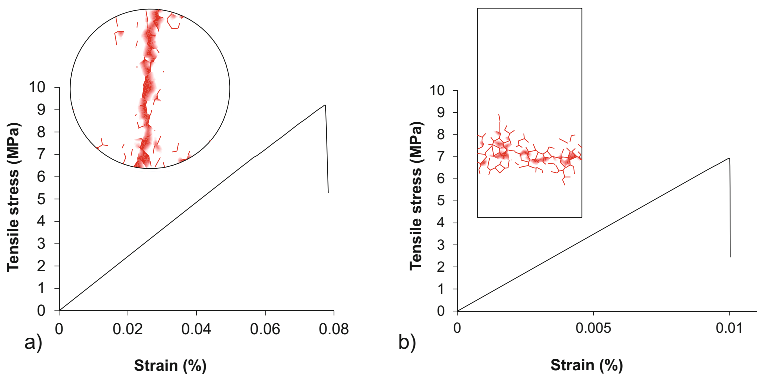

Fig. 4. Simulated stress-strain curves and failure modes in: a) Brazilian; and b) direct tensile tests

3 Influence of Unloading Stress Path on Brittle Damage

3.1 Core Drilling Stress Path

The results of 3D continuum numerical simulations by Martin [3] and Bahrani et al. [2] have shown that during tunnel excavation and core drilling at the 420 level of the URL, the principal stresses constantly change in magnitudes and orientations. They discuss that when the unloading-induced stresses exceed the laboratory-measured crack initiation stress level and/or the tensile strength of intact rock, damage in the form of micro-cracks forms. Bahrani et al. [2] simulated the core drilling process for two borehole orientations using a continuum numerical program with an in-situ stress state representing the 420 level of the URL. Figure 5a and Fig. 5b show the 3D coring stress paths for boreholes parallel to the σ_3 (vertical borehole) and σ_1 (horizontal borehole) directions, respectively. Bahrani et al. [2] applied their simplified stress paths (grey arrows in Fig. 5a and Fig. 5b) to a discontinuum model previously calibrated to the properties of undamaged LdB granite to simulate core damage in the form of micro-cracks.

The simplified stress paths by Bahrani et al. [2] (grey arrows in Fig. 5a) only covered the σ_3 reduction in the compressive zone; it did not account for the tensile stresses generated during core drilling. In this research, first, the simplified stress paths adopted by Bahrani et al. [2] were applied to the calibrated RS2-VTM. To this end, σ_1 and σ_3 values were applied to the model as a stress boundary, while the lower model boundary was fixed in the horizontal direction (Fig. 6a). Figure 6b and Fig. 6c show the simulated damage (i.e., yielded joint elements) for two borehole orientations, representing micro-cracks, which are subparallel to the σ_1 direction. The results of simulations using RS2-VTM in terms of micro-crack orientation agree well with those of discontinuum models by Bahrani et al. [2].

In the preceding step, the calibrated RS2-VTM was subjected to the simplified stress paths by Bahrani et al. [2] for comparison and model verification. In the next step, a revised stress path for the case of a vertical borehole was applied to the calibrated RS2-VTM. As can be seen in Fig. 7a, the revised stress path accounts for the induced tensile

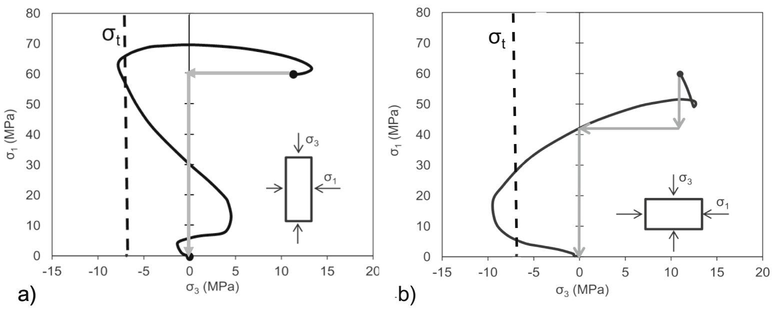

Fig. 5. 3D coring stress path (black curves) for boreholes parallel to: a) σ_3; and b) σ_1 directions [2]. Grey arrows are the simplified stress paths applied to the numerical specimens

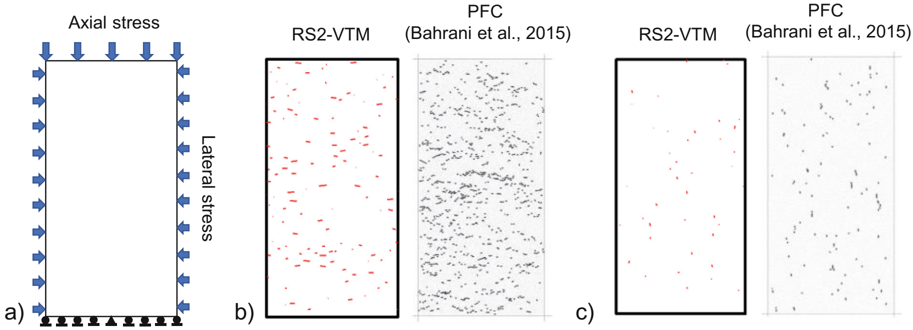

Fig. 6. a) Boundary conditions to apply coring stress path to the calibrated RS2-VTM. Simulated core damage for: b) a vertical borehole after applying the stress path shown in Fig. 5a; and c) a horizontal borehole after applying the stress path shown in Fig. 5b

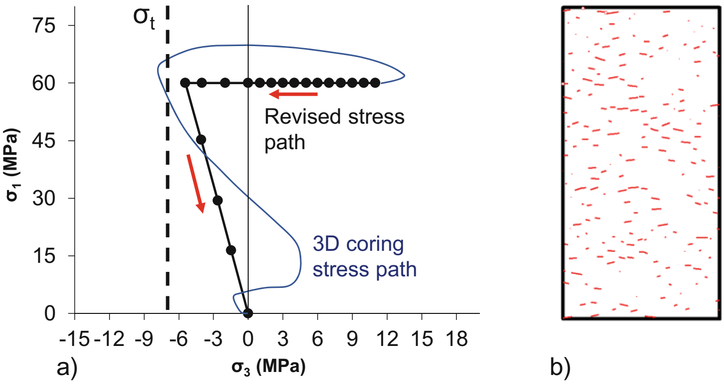

Fig. 7. a) Revised core drilling stress path for a vertical borehole; b) simulated damage due to the application of the revised coring stress path

stresses, i.e., it captures the reduction in σ_3 in the compressive zone and the generation of tensile stresses within the core during drilling before reaching zero stress.

It should be noted that the calibrated RS2-VTM could withstand a maximum tensile stress of 5.4 MPa; for higher tensile stresses, the finite element model failed to converge. Compared to the initial stress path (grey arrow in Fig. 5a), the revised stress path resulted in more damage (i.e., yielded joint elements) in RS2-VTM (Fig. 6b vs Fig. 7b).

3.2 Tunnel Excavation Stress Path

In the next step, the calibrated RS2-VTM was used to investigate the difference between the level of damage associated with 2D and 3D tunnel excavation stress paths. Figure 8a shows the 2D and 3D stress paths for a point in the roof of the MBE tunnel, where the induced compressive stress is 169 MPa. These stress paths were applied to the calibrated RS2-VTMs. Note that stress rotation was not considered in the applied stress paths. In

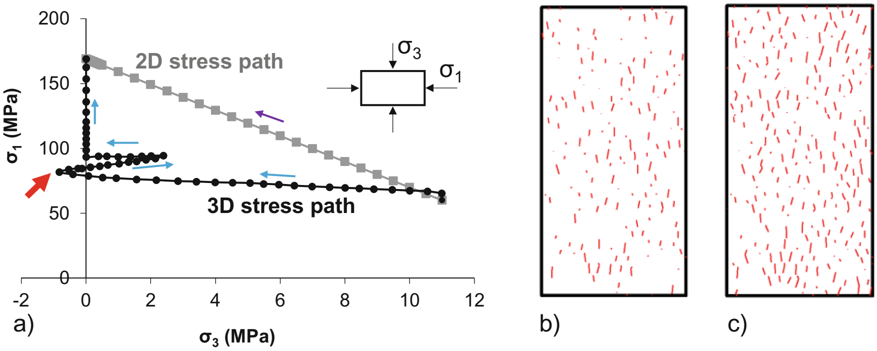

Fig. 8. a) Comparison between 2D and 3D tunnel excavation stress paths. Damaged specimens after applying: b) 2D; and c) 3D tunnel excavation stress paths

these simulations, it was assumed that the long axis of the specimen is parallel to the σ_1 direction. Therefore, σ_1 and σ_3 were applied to the top boundary and sides of the model (see the insert in Fig. 8a). Figure 8b and Fig. 8c depict the simulated damage (i.e., yielded joint elements) associated with the application of 2D and 3D tunnel excavation stress paths, respectively.

As can be seen in Fig. 8b and Fig. 8c, the yielded joint elements, representing micro-cracks, are sub-parallel to the σ_1 direction (specimen long axis). The impact of tensile stress on damage at the tunnel boundary is noticeable when comparing the level of damage (density of yielded joint elements) caused by the 2D and 3D stress paths applied to the calibrated RS2-VTM. The number of yielded joint elements generated by the 2D stress path (Fig. 8b) is less than that of the 3D stress path (Fig. 8c). Therefore, as discussed by Bahrani et al. [9], a higher strength degradation is expected in a 3D model than in a 2D model. This provides further evidence for pre-conditioning (weakening) of the rock mass ahead of the MBE tunnel face, which led to the progressive failure and eventually the formation of a v-shaped notch in the roof and floor of the tunnel [3]. Note that Fig. 8c corresponds to the stress state shown with the red arrow in Fig. 8a.

4 Summary and Conclusions

The Voronoi joint network in RS2 was utilized to generate an RS2-VTM. The model was calibrated against the laboratory properties of undamaged LdB granite. The laboratory test simulation results, including the peak strength and post-peak response, were comparable to those of LdB granite. Next, simplified 3D core drilling stress paths obtained from 3D continuum elastic models were applied to the calibrated RS2-VTM for boreholes: a) parallel to the σ_1 direction, and b) parallel to the σ_3 direction. The simulation results, in terms of micro-crack orientation, were found to be consistent with those of discontinuum models. Finally, 2D and 3D tunnel excavation stress paths were applied to the calibrated RS2-VTM. It was found that the 3D stress path results in more damage, simulated as yielded joint elements in RS2, compared to the 2D stress path, due to the induced tensile stresses generated near the face of an advancing tunnel.

Acknowledgement. The financial support by NSERC and Dalhousie University is acknowledged. This research was also supported by Rocscience through the Rocscience Education Program.

References

1. Martin, CD., Stimpson, B.: The effect of sample disturbance on the laboratory properties of Lac du Bonnet granite. Canadian Geotechnical Journal 31, 692–702 (1994).
2. Bahrani, N., Valley, B., Kaiser, PK.: Numerical simulation of drilling-induced core damage and its influence on mechanical properties of rocks under unconfined condition. International Journal of Rock Mechanics and Mining Sciences 80, 40–50 (2015).
3. Martin, CD.: Seventeenth Canadian Geotechnical Colloquium: The effect of cohesion loss and stress path on brittle rock strength. Canadian Geotechnical Journal 34, 698–725 (1997).
4. Lan, H., Martin, CD., Hu, B.: Effect of heterogeneity of brittle rock on micromechanical extensile behavior during compression loading. Journal of Geophysical Research Solid Earth 115 (B1), (2010).
5. Martin, CD.: Strength of massive Lac du Bonnet granite around underground openings. PhD thesis, University of Manitoba, Alberta (1993).
6. Sanipour, S., Bahrani, N., Corkum, A.: Simulation of Brittle Failure Around Canada's Mine-By Experiment Tunnel Using 2D Continuum-Based Voronoi Tessellated Models. Rock Mechanics and Rock Engineering 55(10), 6387–6408 (2022).
7. Liu, J., Chen, L., Wang, C., Man, K., Wang, L., Wang, J., Rui, S.: Characterizing the mechanical tensile behavior of Beishan granite with different experimental methods. International Journal of Rock Mechanics and Mining Sciences 69, 50–58 (2014).
8. ISRM.: Suggested methods for determining tensile strength of rock materials. International Journal of Rock Mechanics and Mining Sciences and Geomechanics Abstracts 15(3), 99–103 (1978).
9. Bahrani, N., Valley, B., Kaiser, PK.: Influence of stress path on stress memory and stress fracturing in brittle rocks. Canadian Geotechnical Journal 56(6), 852–867 (2019).